

ASCA Observation of a Radio-Loud Quasar and a New Candidate for a Cluster of Galaxies

Fumie AKIMOTO,¹ Akihiro FURUZAWA,¹ Yuzuru TAWARA,¹ Yuichi KAMATA^{1,2}
and
Koujun YAMASHITA¹

¹*Department of Physics, Nagoya University, Furo-cho, Chikusa-ku, Nagoya 464-8602*

²*Research Center for Advanced Energy Conversion, Nagoya University*

Furo-cho, Chikusa-ku, Nagoya 464-8603

E-mail (FA): akimoto@u.phys.nagoya-u.ac.jp

(Received 1999 June 14; accepted 1999 August 19)

Abstract

During an X-ray observation of the distant galaxy cluster CL 0107+31 ($z = 0.69$) with ASCA, an extended X-ray source was detected in the field of view. Based on an image analysis in two different energy bands of 1–3 keV and 3–10 keV, we found that this source consists of a hard point-like component and an additional soft diffuse X-ray source extended over $\geq 3'$ in radius. However, due to poor photon statistics, we could not distinguish whether their X-ray spectra are thermal or non-thermal. The peak position of the central X-ray source coincides with a radio-loud quasar, NRAO 58. NRAO 58 is found to have a power-law spectrum with a photon index $1.6_{-0.2}^{+0.3}$ and a (2–10 keV) luminosity of $\sim 4 \times 10^{46}$ erg s⁻¹ (in the quasar rest frame). The extended component is likely to be a candidate for a nearby galaxy group which accidentally coincides with the quasar.

Key words: galaxies: clusters: individual (CL 0107+31) — galaxies: individual (NRAO 58) — X-rays: galaxies

1. Introduction

NRAO 58 is a radio galaxy whose integrated flux density at 4.75 GHz is 270 mJy (Neumann et al. 1994). The optical counterparts were identified in both *B* (18.2 mag) and *R* (17.4 mag) images in APM and USNO catalogues of the Space Telescope Science Institute (STScI), and located at the position of ($\alpha_{J2000} = 01^{\text{h}}09^{\text{m}}27^{\text{s}}.9$, $\delta_{J2000} = +31^{\circ}49'56''$). Laurent-Muehleisen et al. (1998) identified this object as a radio-loud quasar, RGB J0109+318, with redshift of 1.71.

An X-ray source, which coincides with the object, was also detected during the ROSAT All Sky Survey (RX J0109.4+3149, Brinkmann et al. 1997). The position of the X-ray peak was determined to be ($\alpha_{J2000} = 01^{\text{h}}09^{\text{m}}27^{\text{s}}.7$, $\delta_{J2000} = +31^{\circ}49'57''$), which coincides with NRAO 58.

We report on the X-ray properties of this source based on data obtained from an ASCA observation. This paper comprises five sections. In section 2 we describe the details of the observation. The results and the discussions are presented in section 3 and section 4, respectively. A summary of this paper is given in section 5. Throughout this paper we use the solar abundances given by Anders

and Grevesse (1989), $H_0 = 50$ km s⁻¹ Mpc⁻¹ and $q_0 = 0$, and the quoted errors are the 90% confidence level.

2. Observations

Figure 1 shows an X-ray image obtained from ASCA observations, emphasizing the relative position to a cluster of galaxies, CL 0107+31 (3C 34). As can be clearly seen, the X-ray source including NRAO 58 (the west peak) is much brighter than CL 0107+31 (the east peak). This X-ray image was obtained during an observation of CL 0107+31 on January 11–14 in 1997; when the center of the field of view (FOV) was located at the primary target CL 0107+31, the source including NRAO 58 was detected near to the edge of the gas-imaging spectrometer (GIS) FOV, and was thus not in the solid-state imaging spectrometer (SIS), which had been operated with 1 CCD mode [see Ohashi et al. (1996) and Makishima et al. (1996), Burke et al. (1994) for details of GIS and SIS, respectively. Regarding the X-ray telescopes of ASCA (XRTs), see Serlemitsos et al. (1995)].

A supplementary observation was carried out while focusing on a bright X-ray source including NRAO 58, 6 months later, on July 21–22 in 1997, both with the

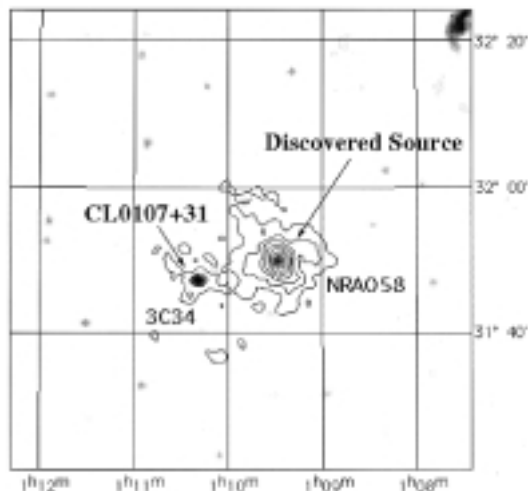


Fig. 1. ASCA GIS 2+GIS 3 X-ray contour in the 0.7–10 keV band of both observations for a serendipitously detected X-ray source detected near the distant rich compact cluster of galaxies CL 0107+31 surrounding a bright radio galaxy; 3C 34 ($z = 0.69$). The image has been smoothed with a Gaussian profile having a width of $\sigma = 0'.5$, and the contour levels are logarithmically spaced with a lowest level of 2×10^{-4} cts s^{-1} arcmin $^{-1}$. The superposed gray scale shows a 1.4 GHz radio image obtained from the NRAO VLA Sky Survey (NVSS) project, whose the beam size = $45''$ (FWHM) resolution

GIS and the SIS. The GIS data were taken in the nominal PH mode throughout the observations with a circular field of $25'$ radius, while the SIS data were taken in the 2 CCD mode covering a FOV of $11' \times 22'$. The effective exposure time of these two observations were ~ 66 ks during the first period and ~ 24 ks for the second period, respectively.

In both observations, steady X-ray emission from CL 0107+31 was detected with counting rates of ~ 0.002 cts s^{-1} in each GIS within a circle of $5'$ radius in the 0.7–10 keV energy band and in each SIS within a circle of $3'$ radius in the 0.5–10 keV energy band. The counting rate of the source including NRAO 58 was estimated to be ~ 0.016 cts s^{-1} for the GIS within a circle of $3'.5$ radius centered at the peak of the X-ray image in the 0.7–10 keV energy band in the first observational period, and ~ 0.018 cts s^{-1} in the second observational period. The SIS counting rate was estimated to be ~ 0.027 cts s^{-1} in the same region as that covered by the GIS in the 0.5–10 keV energy band, which is consistent with that of the GIS.

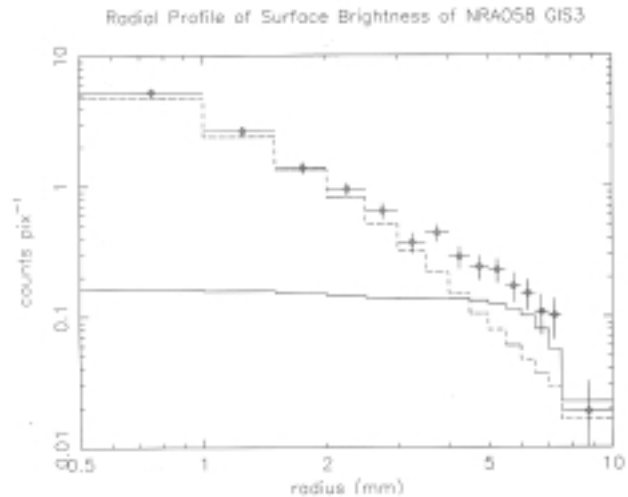


Fig. 2. Radial profile of the surface brightness per detector in the energy range of 1–3 keV, marked as crosses. The error of each data point is 1σ , including the background uncertainty. The dashed and solid lines represent profiles which are expected from simulations for a point source and a uniform diffuse component, respectively.

3. Results

3.1. Counterparts of the X-Ray Source

Two distinct X-ray sources are shown in figure 1. The east weak X-ray source corresponds to the cluster of galaxies CL 0107+31 surrounding the central radio galaxy 3C 34, while the position of the west bright X-ray source is $(01^{\text{h}}09^{\text{m}}5, +31^{\circ}49')$ _{J2000}, which coincides with the radio-loud quasar, NRAO 58 within $1'$, the typical positional error of ASCA (Tanaka et al. 1994). No other identified sources have been found in this field.

3.2. Radial Distribution of X-Ray Surface Brightness

Figure 2 shows the background-subtracted radial profile of the X-ray source centered on NRAO 58 in the energy band of 1–3 keV. The background data were extracted from public-released blank-sky data maintained by ASCA Guest Observer Facility at NASA/GSFC, and were normalized by the effective exposure time. This background is consistent with the background level, which was estimated from the source-free region in our data.

For a comparison with the radial profile, a model profile of a point-source, that is, XRT Point Spread Function (PSF), was produced by an XRT raytracing simulation assuming 2 keV monochromatic X-rays (Tsusaka et al. 1995). Within $3'$ radius from the peak, the radial profile is well fitted by a single point source.

On the other hand, excess extended emission can be seen at larger radii. This result is affected by the background uncertainty, which consists of two origins. One comes from the use of blank-sky data as background; the other comes from the difference between the simulated PSF and the actual PSF. From an analysis of the background using 10 ks observations (Ikebe 1995), the uncertainty of the GIS background for our observation can be estimated to be 0.04 cts/pix (a pixel size is $0'.25 \times 0'.25$). The uncertainty of PSF at $5'$ apart from the X-ray peak is less than 20%. Then, the uncertainty of the surface brightness is estimated to be 0.02 cts/pix. Since the surface brightness of the excess emission was obtained to be 0.13 cts/pix at $5'$ off from the X-ray peak, the source shows a significant excess over that of a point source. Unfortunately, the uncertainty of the SIS background is very large (factor of ~ 2) and can not be estimated exactly. The central point-like emission has a harder X-ray spectrum than the extended component (see subsection 3.4). To avoid contamination by the hard component, the image obtained in the 1–3 keV energy band was used to investigate the extended component.

To describe the outer tail of the radial profile, we fitted the measured profile within a $7'$ radius to a model which consists of a point-source and a diffuse component. Because of insufficient photon statistics, the diffuse component was assumed to have a flat brightness distribution with a cutoff radius of $7'$. For a single point-source model a fit to the radial profile, using combined data of the first and second observations, resulted in a χ^2 value of 196 (d.o.f. = 54). Adding a diffuse component to the point source model gives a much better fit: the χ^2 value reduces to 63 (d.o.f. = 53), and the resultant flux of the diffuse component is $23 \pm 5\%$ of the total flux.

The source was also detected accidentally at the edge of the ROSAT PSPC ($43'$ apart from the center) in a 27 ks pointed observation, with a counting rate of 0.05 cts s^{-1} . However, the uncertainties of the background level and the point spread function at such large off axis angles prevent us from examining the extent of the source. (We obtained these data from the public archive through the HEASARC on-line service provided by NASA/GSFC.)

3.3. Temporal Analysis

To investigate changes in the X-ray flux between two observational periods, we compared the fluxes within a circle of $7'$ radius centered at the peak of the source including NRAO 58, taking into account vignetting corrections in each observation; also, the counting rates of the background were estimated from the source-free regions in the same field of view. The X-ray flux during the follow up observation was 30% smaller than that of the first observation in the energy band of 0.7–10 keV, which is significant at the 4σ level. Unfortunately, the poor

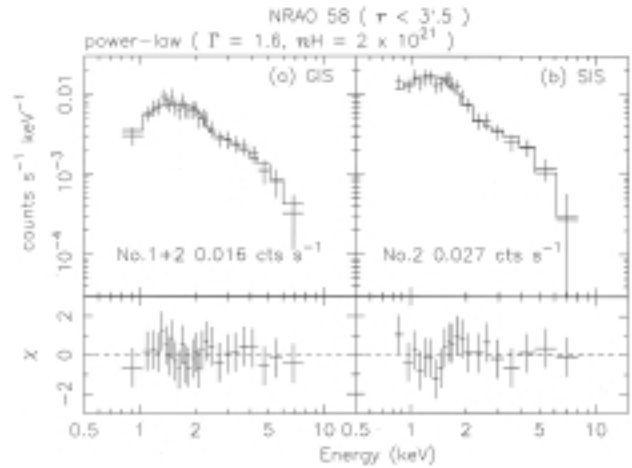


Fig. 3. (a) GIS 2+GIS 3 spectrum from a circular region with a radius of $3'.5$ obtained during two observation periods. In the top panel, we show the data and the best fit power law model (with photon index 1.60 and $nH = 2 \times 10^{21} \text{ cm}^{-2}$). The lower panels are residuals from the best-fit model in units of σ . (b) SIS 0+SIS 1 spectrum obtained during the second observation period, fitted with the same model.

photon counts do not allow us to distinguish whether the change originates from the central source or the extended source.

3.4. Spectral Analyses

For spectral analyses, we accumulated GIS 2+GIS 3 spectra for three regions: within a circle of $3'.5$ and $7'.0$ radius centered on the X-ray peak, and an annulus of $3'.5$ – $7'.0$ radius, while we made SIS 0+SIS 1 spectra within a circle of $3'.5$ radius. The data in the regions outside the $7'$ circle were used to estimate the background spectrum.

In spite of the existence of extended emission, these spectra show no significant emission lines. Therefore, we cannot estimate the redshift of this source from the X-ray data. We then fitted the GIS and SIS spectra simultaneously, assuming a single power law and absorption hydrogen column density nH with galactic value ($6.1 \times 10^{20} \text{ cm}^{-2}$) (Heiles 1975). The best-fit parameters are summarized in table 1. At a $z = 1.71$, the luminosities in the observed 2–10 keV band are also listed. The resulting spectra are shown in figure 3. The photon index of 1.5–2.0 is typical among AGNs. It is also noted that the photon index of the spectrum within $r < 3'.5$ is smaller than that in the outer region. This trend is not due to an inappropriate choice of the amount of absorption, since it held even when we used the galactic absorption value (see the last column of table 1): The inner region seems to be harder than the outer region.

Table 1. Best-fit parameters of power law model.

Radius arcmin	Photon index	nH 10^{22} cm^{-2}	$F_{X2-10\text{keV}}$ $\text{erg s}^{-1} \text{ cm}^{-2}$	$L_{X2-10\text{keV}}$ erg s^{-1}	χ^2_ν	Photon index*
0–7.0	$1.8^{+0.2}_{-0.2}$	$0.19^{+0.23}_{-0.19}$	$1.4^{+0.6}_{-0.4} \times 10^{-12}$	$6.1^{+2.6}_{-1.8} \times 10^{46}$	0.39	$1.7^{+0.1}_{-0.2}$
0–3.5	$1.6^{+0.3}_{-0.2}$	$0.17^{+0.16}_{-0.14}$	$1.2^{+0.5}_{-0.5} \times 10^{-12}$	$5.2^{+2.2}_{-2.2} \times 10^{46}$	0.29	$1.5^{+0.1}_{-0.1}$
3.5–7.0	$2.0^{+0.5}_{-0.5}$	0.061 fixed	$4.4^{+1.5}_{-1.3} \times 10^{-13}$	$1.9^{+0.7}_{-0.6} \times 10^{46}$	0.16	$2.0^{+0.5}_{-0.5}$

*Value at $nH = 6.1 \times 10^{20} \text{ cm}^{-2}$.

4. Discussion

4.1. The Point Source NRAO 58; A Radio-Loud Quasar

NRAO 58 was detected in the ROSAT survey and at the edge of the detector during a ROSAT PSPC pointing observation. The ROSAT flux in the 0.1–2.4 keV energy band was estimated to be 1.60×10^{-12} (Neumann et al. 1994) and $(1.41 \pm 0.33) \times 10^{-12} \text{ erg s}^{-1} \text{ cm}^{-2}$ (Laurent-Muehleisen et al. 1998; Brinkmann et al. 1997).

The ASCA total flux in the observed 2–10 keV band is $1.4^{+0.6}_{-0.4} \times 10^{-12} \text{ erg s}^{-1} \text{ cm}^{-2}$ in $r < 7'$ (see in table 1). The X-ray flux in the 0.1–2.4 keV energy band is estimated to be $1.8^{+0.8}_{-0.5} \times 10^{-12} \text{ erg s}^{-1} \text{ cm}^{-2}$ from an extrapolation of the ASCA X-ray spectrum assuming a single power law with a photon index of 1.8.

The X-ray spectrum of the point-like component was reproduced by a single power law with a photon index of $1.6^{+0.3}_{-0.2}$, which dominates the X-rays coming from the inner region of the X-ray source, which is a typical value for AGNs. The X-ray flux and the luminosity in the 1–3 keV energy band ($r < 7'$) are estimated to be $5.5^{+1.8}_{-2.9} \times 10^{-13} \text{ erg s}^{-1} \text{ cm}^{-2}$ and $2.4^{+1.3}_{-0.8} \times 10^{46} \text{ erg s}^{-1}$, respectively, which correspond to 72–82% of the total flux within $7'$. Even with this reduced X-ray flux, the obtained flux ratio $\log(f_X/f_V)$ of ~ -3 is typical for a radio-loud quasar.

4.2. The Diffuse Component; A Group or Cluster of Galaxies?

Since no significant emission line was detected in the X-ray spectrum, it has not been determined whether the emission is thermal or non-thermal. The spatial extent of the X-ray source indicates that it neither originates in the X-ray halo of a relatively nearby galaxy nor is a galactic source, such as a supernova remnant. We searched for counterparts of the diffuse X-ray source using the SIMBAD database with $7'$ radius of the X-ray center, and could find no candidate, except for a catalog object corresponding to the central radio object, RX J0109.4 – 3149, RGB J0109 + 318, and EF B0166 + 3134. The high galactic latitude of -30.9 suggests only a small possibility of

a chance coincidence with galactic objects. Thus a group or a cluster of galaxies is a likely candidate of this X-ray source. At $z = 1.71$, the X-ray luminosity in the 2–10 keV energy band, temperature, and metal abundance are estimated to be 5^{+13}_{-2} keV , $0.8 (< 3)$ solar abundance, and $1.0^{+0.2}_{-0.1} \times 10^{46} \text{ erg s}^{-1}$ in the rest frame. This X-ray luminosity is similar to that of the largest rich clusters.

Optical imaging observations (V , R , I bands) of this region have been conducted at Kitt Peak Observatory, by Nakahira et al. (1999, unpublished). They claimed that, though there is no evidence for the existence of a rich galaxy cluster, there are several small concentrations of nearby galaxies ($z \sim 0.1$) in the field of view. According to this result, a large redshift of 1.71 is unlikely.

For $z = 0.1$, the temperature and the X-ray luminosity would be $2.9^{+5.8}_{-1.8} \text{ keV}$ and $8.5^{+2.2}_{-1.7} \times 10^{42} \text{ erg s}^{-1}$, respectively. In this case, the temperature and the X-ray luminosity are typical for a group of galaxies or a poor cluster of galaxies. It is suggested that the diffuse X-ray component is from a nearby group of galaxies or a poor cluster of galaxies ($z \sim 0.1$) and accidentally coincides with the position of NRAO 58.

5. Summary

A diffuse X-ray source was found in the ASCA GIS FOV during an observation in 1997 January. The position of the source was determined to be ($\alpha_{J2000} = 01^{\text{h}}09^{\text{m}}28^{\text{s}}$, $\delta_{J2000} = +31^{\circ}49'21''$). Within the ASCA error circle of the position, it is coincident with a radio-loud quasar, NRAO 58.

The surface-brightness distribution within a circle of $7'$ radius can be reproduced by the combination of a point-like component and a diffuse component (23% of the total X-ray flux). The central point-like source is consistent with a radio-loud quasar from the SED. On the other hand, we could not distinguish whether the diffuse component is of thermal or non-thermal origin. Due to the absence of any optical counterparts in this region, except for the central object and the high galactic latitude, the diffuse X-ray source is a candidate of X-ray emitting cluster of galaxies. Several concentrations

of nearby galaxies ($z \sim 0.1$) in this region during the optical photometry at Kitt Peak Observatory support this hypothesis.

Future X-ray missions with better spatial and energy resolutions, such as Astro-E, AXAF, and XMM, are expected to clarify whether the diffuse component is truly a group or cluster of galaxies. Similarly, optical redshifts are desired to determine the cluster properties.

We thank the ASCA team for their daily operation of ASCA and SimASCA software team. We also thank Y. Kumai, M. Tanaka, K. Ohta, M. Matsumura, M. Arnaud, and H. Watarai for their useful advice and help. This research is made possible with the use of five databases; the NASA/IPAC Extragalactic Database which is maintained by the Jet Propulsion Laboratory, California Institute of Technology, the Digitized Sky Survey database provided by the Space Telescope Science Institute (STScI), the National Radio Astronomy Observatory VLA Sky Survey database, SIMBAD astronomical database maintained by CDS, Strasbourg, and ROSAT image database of the HEASARC on-line service provided by NASA/GSFC.

References

- Anders E., Grevesse N. 1989, *Geochim. Cosmochim. Acta* 53, 197
- Brinkmann W., Siebert J., Feigelson E.D., Kollgaard R.I., Laurent-Muehleisen S.A., Reich W., Fürst E., Reich P. et al. 1997, *A&A* 323, 739
- Burke B.E., Mountain R.W., Daniels P.J., Cooper M.J., Dolat V.S. 1994, *IEEE Trans. Nucl. Sci.* 41, 375
- Heiles C. 1975, *A&AS* 20, 37
- Ikebe Y. 1995, PhD Thesis, The University of Tokyo
- Laurent-Muehleisen S.A., Kollgaard R.I., Ciardullo R., Feigelson E.D., Brinkmann W., Siebert J. 1998, *ApJS* 118, 127
- Makishima K., Tashiro M., Ebisawa K., Ezawa H., Fukazawa Y., Gunji S., Hirayama M., Idesawa E. et al. 1996, *PASJ* 48, 171
- Neumann M., Reich W., Fürst E., Brinkmann W., Reich P., Siebert J., Wielebinski R., Trümper J. 1994, *A&AS* 106, 303
- Ohashi T., Ebisawa K., Fukazawa Y., Hiyoshi K., Horii M., Ikebe Y., Ikeda H., Inoue H. et al. 1996, *PASJ* 48, 157
- Serlemitsos P.J., Jalota L., Soong Y., Kunieda H., Tawara Y., Tsusaka Y., Suzuki H., Sakima Y. et al. 1995, *PASJ* 46, 105
- Tanaka Y., Inoue H., Holt S.S. 1994, *PASJ* 47, L37
- Tsusaka Y., Suzuki H., Yamashita K., Kunieda H., Tawara Y., Ogasaka Y., Uchibori Y., Honda H. et al. 1995, *Appl. Opt.* 34, 4848